The International Archives of the Photogrammetry, Remote Sensing and Spatial Information Sciences, Volume XLIV-4/W3-2020, 2020
5th International Conference on Smart City Applications, 7–8 October 2020, Virtual Safranbolu, Turkey (online)

POST-EARTHQUAKE 3D BUILDING MODEL (LOD2) GENERATION FROM UAS IMAGERY: THE CASE OF VRISA TRADITIONAL SETTLEMENT, LESVOS, GREECE.

K. Chaidas[1], G. Tataris[1], N. Soulakellis[1]

[1] Dept. of Geography, University of the Aegean, Mytilene, Greece - k.chaidas@aegean.gr, tataris@geo.aegean.gr, nsoul@aegean.gr

KEY WORDS: UAS, 3D building modelling, LOD2, post-earthquake

ABSTRACT:

In recent years 3D building modelling techniques are commonly used in various domains such as navigation, urban planning and disaster management, mostly confined to visualization purposes. The 3D building models are produced at various Levels of Detail (LOD) in the CityGML standard, that not only visualize complex urban environment but also allows queries and analysis. The aim of this paper is to present the methodology and the results of the comparison among two scenarios of LOD2 building models, which have been generated by the derivate UAS data acquired from two flight campaigns in different altitudes. The study was applied in Vrisa traditional settlement, Lesvos island, Greece, which was affected by a devastating earthquake of Mw=6.3 on 12th June 2017. Specifically, the two scenarios were created by the results that were derived from two different flight campaigns which were: i) on 12th January 2020 with a flying altitude of 100 m and ii) on 4th February 2020 with a flying altitude of 40 m, both with a nadir camera position. The LOD2 buildings were generated in a part of Vrisa settlement consisted of 80 buildings using the footprints of the buildings, Digital Surface Models (DSMs), a Digital Elevation Model (DEM) and orthophoto maps of the area. Afterwards, a comparison was implemented between the LOD2 buildings of the two different scenarios, with their volumes and their heights. Subsequently, the heights of the LOD2 buildings were compared with the heights of the respective terrestrial laser scanner (TLS) models. Additionally, the roofs of the LOD2 buildings were evaluated through visual inspections. The results showed that the 65 of 80 LOD2 buildings were generated accurately in terms of their heights and roof types for the first scenario and 64 for the second respectively. Finally, the comparison of the results proved that the generation of post-earthquake LOD2 buildings can be achieved with the appropriate UAS data acquired at a flying altitude of 100 m and they are not affected significantly by a lower one altitude.

1. INTRODUCTION

Earthquake is one of the most devastating natural disasters that can cause casualties, extended damages on infrastructures (e.g. buildings) and financial loss. According to the Disaster Management Cycle, there are two stages (except the one during the disaster) of strategies which are, the “Ex-Ante” and the “Ex-Post” Strategies (Gutmann, 2011; Government of Japan et al., 2012). The “Ex-Ante” strategies are conducted before a disaster and the “Ex-Post” Strategies after a disaster. The Ex-Post Strategies include post-disaster phases which are response, recovery and reconstruction (Khan et al., 2008). It is clear that when an earthquake occurs, the obtaining information for the damage assessment is important (Xu et al., 2014). As Letellier et al. (2007) compiled, the post-earthquake recording of cultural heritage buildings is significant. After an earthquake, the damage assessment of the buildings is still made through fieldwork, however, these traditional methods are time-consuming, and sometimes dangerous due to the extensive damages (Chatzistamatis et al., 2018).

Remote sensing techniques can cover large areas and proved to be very effective and accurate for the acquisition of disaster information (Dominici et al., 2017). These techniques are useful for mapping the affected area after an earthquake and for monitoring during the recovery and reconstruction phase as well. Over the past few years, UAS (Unmanned Aerial Systems), are widely used for data acquisition after an earthquake and many researches propose that they are very suitable for these cases (Dominici et al., 2017; Tu et al., 2017; Xu et al., 2014). According to Tu et al. (2017), the use of high-resolution aerial imagery for the detection of damaged buildings can support quicker and more efficient decision making in disaster management. As Ma and Qin (2012) compiled, nadir aerial images can depict totally collapsed buildings or damaged roofs.

Nevertheless, the post-earthquake damage assessment of the affected area has mostly been done through 2D mapping and without considering the dimensions of the building (Daniyal, 2012). According to Kim et al. (2016), while remote sensing technology has increased the speed and accuracy of damage mapping at a city scale, challenges remain at more specific per-building levels. According to Yilmaz (2015), nowadays the 3D geo-spatial data visualization is commonly used in Disaster Management, as it allows decision-makers to understand better the disaster phenomena.

3D representation of urban environment is essential in order to better understand our world. In recent years 3D modelling is used in various domains such as navigation, urban planning, cadastre and disaster management (Biljecki et al., 2015). Many approaches for post-earthquake 3D modelling have been made (Maruyama et al., 2011; Daniyal, 2012; Chiabrando et al., 2017; Yamazaki et al., 2017), however one of them is the CityGML standard that is still unexploited.

CityGML is a standard data model format of the Open Geospatial Consortium (OGC) for the representation, storage and exchange of 3D models (Kolbe, 2009; Open Geospatial Consortium, 2012). The CityGML standard defines the geometry, topology, semantics and appearance of objects in 3D at five Levels of Detail (LODs) (Kolbe, 2009). LOD0 is 2.5D footprints, LOD1 is a generalized prismatic block model with walls and flat roof, LOD2 is a model with walls and a various types of roof structure. LOD3 is a detailed model with windows and doors. LOD4 is a LOD3 that includes interior structures (Kolbe, 2009; Tang et al., 2020). After a CityGML conversion of the models, the semantics (attributes) attached to each 3D object allow the implementation of queries. As Kolbe et al. (2005) compiled, thematically rich attributes allow specific queries like 'What are the buildings with more than 10 storeys above ground?' or 'Where are buildings with flat roofs which are large enough that a helicopter could land on them?'.

The aim of this paper is to present the methodology and the results of the comparison among LOD2 buildings using the CityGML standard, which have been generated by the derivate data acquired from two flight campaigns with different flying altitudes. In this study, a workflow is presented for the generation of 3D building models using DSMs and building footprints. There are some approaches in the literature for 3D building modelling using UAS data (Agugiaro, 2014; Buyukdemircioglu et al., 2018). The building reconstruction is made with model-driven method (Zheng and Weng, 2015).

2. MATERIALS AND METHODS

2.1 Study Area

Vrisa's traditional settlement (Figure 1), on the south-eastern coast of Lesvos Island, Greece, was partially destroyed by a devastating earthquake (Mw=6.3) on 12th June 2017 (Kiratzi, 2018; Papadimitriou et al., 2017). The study area is a part of the Vrisa settlement with a 0.022 km² area, that includes 80 buildings with all types of damages. This area was preferred, as it is the centre of the settlement with both commercial land use and urban land use.

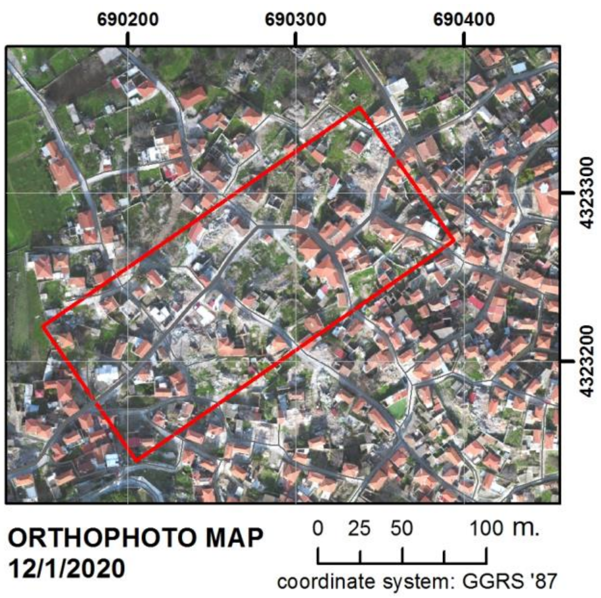

Figure 1. The study area is a part of the Vrisa settlement (0.022 km² area), that includes 80 buildings with all types of damages.

The geological and geomorphological setting along with the characteristics of the buildings are the factors regulating the spatial distribution of the damages on the buildings. Specifically, the combination of old masonry structures founded on alluvial deposits in an area bounded by significant faults in combination with probable directivity phenomena resulted in destruction (Lekkas et al., 2017). Damaged buildings belonging into scales 4 and 5 according to the EMS-98 (European Macroseismic Scale) should be demolished by their owners while all the rest ones should be repaired. Specifically, approximately 340 out of 1100 buildings of Vrisa traditional settlement should be demolished and reconstructed.

On the 13th of June and for one month, a data acquisition campaign from the University of the Aegean took place, for the 3D mapping of Vrisa settlement, as a research project funded by the North Aegean Region. GCPs measurements, UAS nadir and oblique images, terrestrial photographs and terrestrial laser scanner point clouds were obtained for the 3D mapping of Vrisa Settlement at three different spatial scales: i) a village-scale, ii) a street-scale, and iii) a building-scale (Papakonstantinou et al., 2018; Soulakellis et al., 2018).

2.2 Methodology

The workflow of this study, is presented in Figure 2 and consists of five steps: i) the UAS data acquisition, which was consisted of two flights, ii) the photogrammetric processing of the acquired data, iii) the input data that were used, iv) the 3D model generation, where the LOD2 buildings reconstructed and v) the comparison implemented.

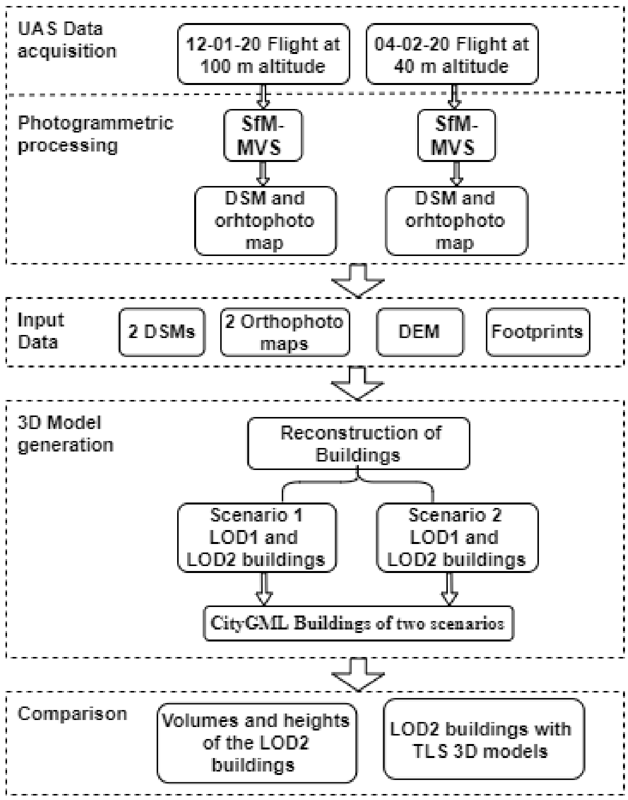

Figure 2. Workflow of the developed method

2.2.1 UAS data acquisition

Two flight campaigns were performed in the study area using a DJI Phantom 4 Pro system. These flights were carried out, for the evaluation of the different altitudes compared to the generation of 3D buildings. Flight planning parameters are presented in Table 1. The first flight was conducted on the 12th January 2020 at 100 m altitude with a nadir field of view. The overlap was set at 80% front overlap and 70% side lap. A total area of 0.152 km² was mapped and the flight time was 10 min. The second flight was conducted on the 4th February 2020 at 40 m altitude with a nadir field of view. The overlap was set at 70% front overlap and 50% side lap. For the second flight, a total area of 0.152 km² was mapped with a flight time of 22 min. The ground resolutions were calculated to be 2.83 cm/pix for the first flight and 2.19 cm/pix for the second. The number of the acquired UAS high-resolution images were 222 for the first flight and 499 for the second.

Flight	Date	12-01-20	04-02-20
	Duration	10 min	22 min
	Altitude	100 m.	40 m.
FOV direction		nadir	nadir
GSD		2.83 cm/pix	2.19 cm/pix
Overlapping of images	Front overlap	80%	70%
	Side lap	70%	50%
Number of images		222	499
Total area		0.152 km²	0.152 km²

Table 1. Flight planning parameters for UAS data acquisition

2.2.2 Photogrammetric processing

The UAS nadir images of the different acquisition dates were processed for the generation of high-resolution orthophoto maps and DSMs using Structure from Motion (SfM) and Multi-View Stereopsis (MVS) algorithms, in Agisoft Metashape Version 1.6 software (Agisoft-LLC, 2020).

The results of the photogrammetric processing were a DSM of 5.65 cm/pix spatial resolution and an orthophoto map of 2.8 cm/pix spatial resolution from the UAS images acquired from the first flight on 12th January 2020 with a flying altitude of 100 m. For the second flight on 4th February 2020 with a flying altitude of 40 m, a DSM of 4.38 cm/pix spatial resolution and an orthophoto map of 2.1 cm/pix spatial resolution were produced.

2.2.3 Input Data

The input data which were used for the 3D modelling are the DSMs and the orthophoto maps derived from the two flight campaigns, a DEM and the footprints of the buildings. The DEM of 10 cm/pix spatial resolution was produced from the topographic survey of 233 GCPs which were measured with the RTK method, that took place during the 3D mapping of Vrisa settlement. Buildings footprints were manually digitized in ArcMap (ESRI) using the orthophoto map that was derived after the earthquake. Thus, these footprints represent the situation of the buildings at the period after the earthquake. All these products were clipped at a 0.022 km² area (of the study area) in order to be utilized for the 3D modelling of the buildings.

2.2.4 3D model generation

In this study, an approach for an automatic generation of 3D buildings from a post-earthquake area has been followed using UAS imagery. BuildingReconstruction 2018 software (BREC) from VirtualCity Systems GmbH, Berlin, Germany have been used for the generation of 3D models. The software requires digital surface and terrain models as well as 2D building footprints and reconstructs valid 3D models in LOD1 and LOD2. DSMs and DEM are required from the software in order to calculate the base height of a building from the terrain.
BREC uses some algorithms to detect the roof shape from the DSM. The cell decomposition algorithm is used for buildings with multiple roof shapes and varying heights (Kada and McKinley, 2009). An integrated library of more than 28 main and connecting roof types is used to detect the best fitting roof type for each produced cell. The rectangle decomposition algorithm is used for simple geometries to be processed with rectangular intersections. Finally, the footprint extrusion algorithm is used to create LOD1 models of large areas and flat LOD2 buildings (Buyukdemircioglu et al., 2018).

BREC uses a model-driven approach to detect and reconstruct the roof geometry and shape according to the library of roof types. The 3D building geometry is reconstructed for each given footprint. The geometry of models is absolutely closed, and it is fully consistent with the building footprint. Furthermore, the software enables manual editing of building geometries in case they are not correct.

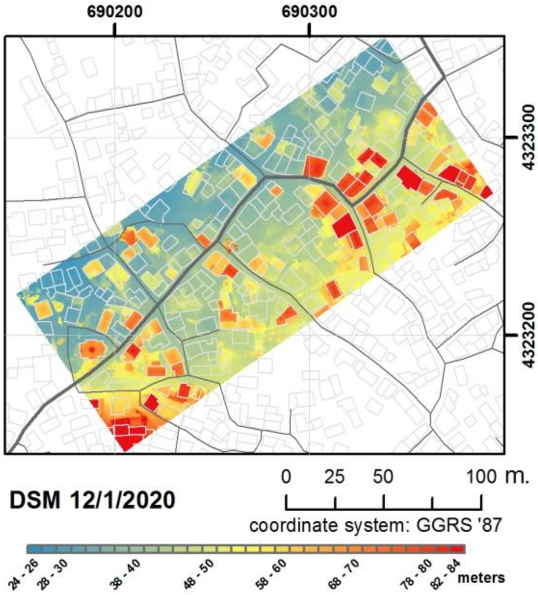

Figure 3. DSM (5.65 cm/pix) derived from the first flight of 100 m altitude

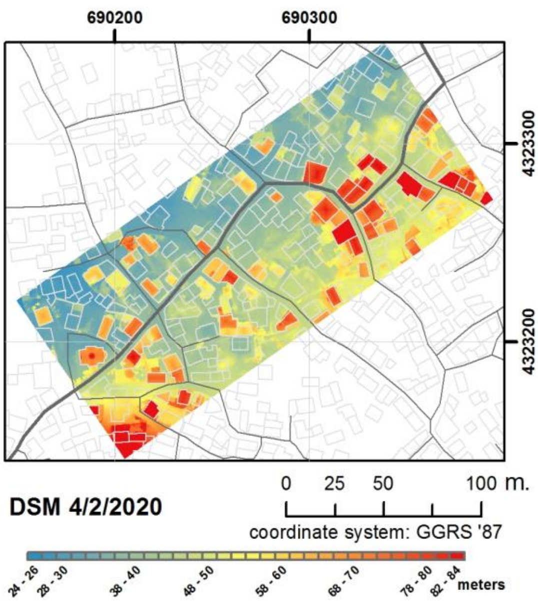

Figure 4. DSM (4.38 cm/pix) derived from the second flight of 40 m altitude

The method was implemented in the study area of the settlement and for the comparison of the different flying altitudes, two scenarios of 3D modelling were implemented. Thus, the same buildings of the same area were reconstructed in LOD2 with the same settings. The scenarios are as follows:

- Scenario 1 was implemented with the DSM of 5.65 cm/pix spatial resolution (Figure 3) and the orthophoto map that were derived from the 1st flight of 100 m altitude, the DEM (10 cm/pix) and the building footprints.
- Scenario 2 was implemented with the DSM of 4.38 cm/pix spatial resolution (Figure 4) and the orthophoto map that were derived from the 2nd flight of 40 m altitude, the DEM (10 cm/pix) and the building footprints.

In Figure 5 are shown the footprints of the 80 buildings, and the LOD2 buildings that were generated in BREC. The input data were pre-processed in the formats that the software requires. The building footprints refer to the area of the building structure (boundaries), were used to determine the geometry of the walls in the building model. The footprints with their attributes (semantics) of the buildings were added and stored in a single ESRI shapefile, giving each building polygon a unique ID. The attributes of the buildings were: building material, number of floors, damage scale, and owner. These attributes can be used to implement queries, after the CityGML conversion of the models. The building footprints were extruded from the DEM up until they reach the DSM. The roof shape is defined as the best fit to an internal catalogue template. This stage produces the geometry of LOD2 models. Finally, the orthophoto maps were used for visual inspection.

BREC 2018 gives the option to export the created LODs directly in CityGML format and add semantic information to the building models. This option was used to export LOD1 and LOD2 models of the buildings. The 3D buildings of the two scenarios were exported as CityGML LOD2 models and each 3D building separately, as 3D object in PLY format for some further transforms.

Figure 5. a) Footprints of 80 buildings used for the 3D reconstruction of the two scenarios and b) LOD2 buildings generated by BuildingReconstruction software

2.2.5 Comparison and evaluation of the LOD2 models

For the estimation of the product's accuracy, the volumes and the heights of the LOD2 buildings of the two scenarios were compared. For each scenario, the volumes of the LOD2 buildings were acquired directly from the BREC software. Subsequently, the heights of the LOD2 buildings were calculated from the building attributes of the BREC. For each building there is available information about the lowest vertex roof and ground level, so the building height is calculated as their difference.

Furthermore, TLS 3D models which were produced during the 3D mapping of the Vrisa settlement (Soulakellis et al., 2018), were compared with some LOD2 buildings visually, for the validation of their location, geometry and height. Finally, some TLS heights were measured, considering their heights as accurate, for further comparison between the LOD2 models and the TLS models.

3. RESULTS AND DISCUSSION

The area that was studied, contains 80 buildings with different shapes and all kinds of damages according to the EMS-98 damage scale and were are all generated using the BuildingReconstruction software. BREC was relatively appropriate for the automatic reconstruction of LOD2 buildings. The software uses model-driven approach to detect and reconstruct the buildings from the necessary input data (DSM, footprints). Buildings with roof types and roof heights that exist in the library with the roof models can be generated accurately. The problem is that the complex roof structures cannot be recognized by the algorithm. On the other hand, the processing of the 3D building reconstruction is very quick, and the buildings have a precise geometry. LOD2 buildings produced, contain semantic information besides the semantics contained in the attributes of the footprints. These semantics are highest vertex for the roof, roof type, lowest vertex of the roof, ground area, ground level, roof type and building volume.

As shown in Table 2, for the first scenario, 75 buildings were reconstructed by cell decomposition, 3 by rectangle decomposition and 2 by extrusion. For the second scenario, 74 buildings were reconstructed by cell decomposition, 3 by rectangle decomposition and 3 by extrusion.

BuildingReconstruction algorithms	Number of Buildings scenario 1	Number of Buildings scenario 2
Cell decomposition	75	74
Rectangle decomposition	3	3
Footprint extrusion	2	3

Table 2: Number of buildings reconstructed from BREC algorithms for each scenario

Most of the buildings in the test area have been generated correctly, according to geometry and roof structure (Figure 6). According to visual inspection, 65 LOD2 buildings for scenario 1 and 64 for scenario 2 have been generated correctly. It was difficult, for the algorithm to recognize the roof structure and shape of some buildings like the church.

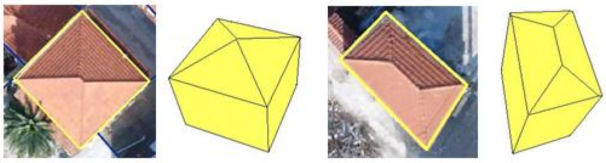

Figure 6. Example of Correct 3D reconstruction of buildings

Some problems must be mentioned for the reconstruction phase of buildings. First of all, this approach concerns the post-earthquake generation of LOD2 buildings, and it is logical that there are several difficulties. Thus, some footprints were added intentionally, for the representation of damaged, demolished and buildings that are being constructed, in order to test their generation. As shown in Figure 7 these LOD2 buildings were generated wrong and the errors are as it follows:

The first building is actually debris and it should be generated as a LOD1 object with a height and volume, but it was generated as a LOD2 building with a roof structure and also different roof shape between the two scenarios. Second and third LOD2 buildings of the figure, have errors in the roof structure between the two scenarios. The last LOD2 building has been generated correct only for scenario 2, as it is being constructed.

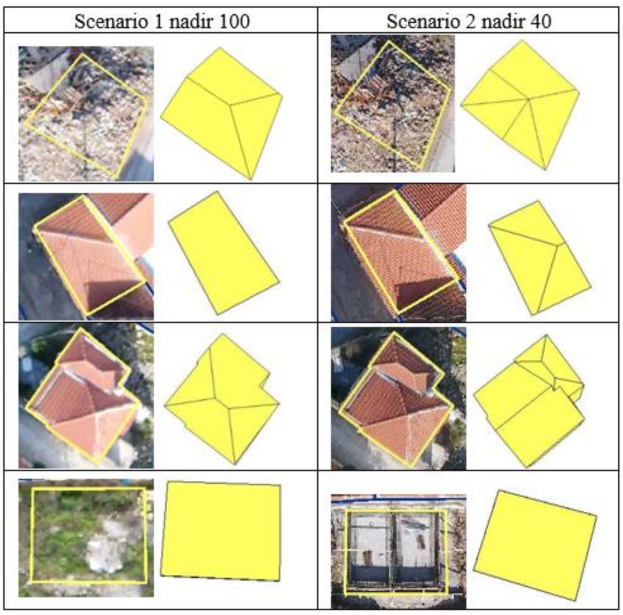

Figure 7. Errors of the 3D reconstruction of some footprints

The visualization of LOD2 buildings (Figure 8) was made in ArcGIS ArcScene and FZK Viewer (KIT). Specifically, the LOD2 buildings were transformed in COLLADA format as separate buildings and were visualized in ArcScene and in CityGML format were rendered in FZK Viewer.

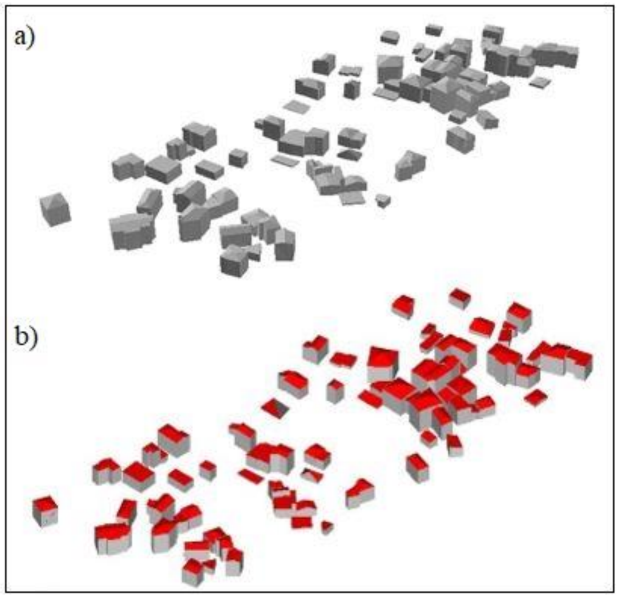

Figure 8. a) Visualization of LOD2 buildings in ArcScene and b) in FZK Viewer

Moreover, CityGML LOD2 models for the two scenarios were illustrated in FME Data Inspector (SAFE SOFTWARE, 2015), to verify the reliability of CityGML models that were produced. As mentioned before, BREC can export the created LOD2 building models directly in CityGML. CityGML LOD2 models are correctly formatted to be classified into RoofSurface, GroundSurface, and WallSurface. The LOD2 buildings were evaluated for the visual and metric qualities through the above software. LOD2 models, reproduce the buildings in a realistic way, and the visual accuracy was sufficient. Semantic information can be queried from the model to search for example a certain type of attribute. 3D visualization of seismic buildings is a very effective tool for further damage management. The 3D representation of a damage affected urban environment can provide a better communication and help in the decision-making process.

In Figure 9, a visual comparison between the volumes of the two scenarios is depicted. The X-axis represents the values of the first scenario while in the Y-axis the values of the second scenario. Ideally, the values of both scenarios should be intersected on the trendline. Outlier values refer to two buildings that are being rebuilt. The two scenarios provide slightly different results. From this figure, it is clearly shown that the two scenarios provide reasonable results. The total volume of the buildings in scenario 1 is 21.720 m3 and in scenario 2 is 22.031. Their difference is 311 m3 which is due to buildings that are rebuilt.

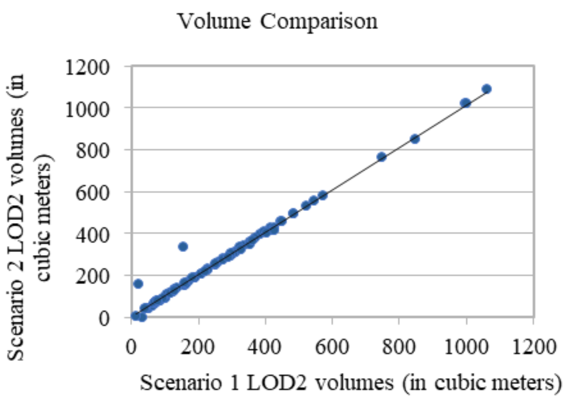

Figure 9. Volume comparison of LOD2 buildings between the two scenarios

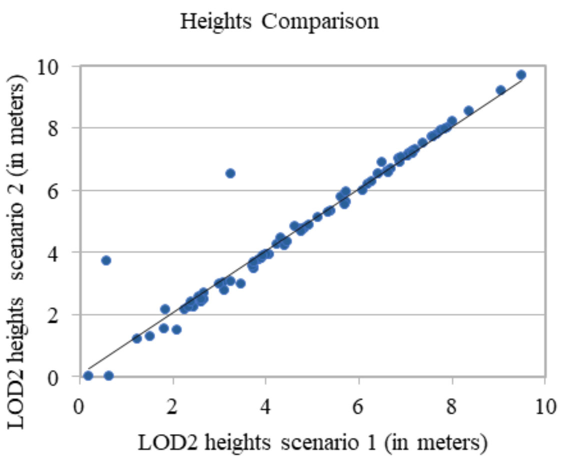

Figure 10. Heights comparison of LOD2 buildings between the two scenarios

Regarding the comparison of the heights, also a visual comparison of the heights between the two scenarios is depicted (Figure 10). The X-axis represents the values of the first scenario while in the Y-axis the values of the second scenario. Ideally, the values of both scenarios should be intersected on the trendline. Again, outlier values refer to buildings that are being rebuilt. The two scenarios provide slightly different results.
From this figure, it is clearly shown that the two scenarios provide reasonable results. Two buildings have different heights in the two scenarios. In detail, a building's height is 3.25 m for scenario 1 and 6.54 m for scenario 2. This is due to the rebuilding of the building during the first flight of 100 m altitude (scenario 1). A month later, at the second flight of 40 m altitude, the building was completed. Another building had a height of 0.57 m during the period of the first flight and a height of 3.72 m during the period of the second, as it was rebuilt too.

For further analysis, the heights of the buildings were compared with available TLS 3D models. First, for visual inspection, the LOD2 buildings and the TLS models were imported in CloudCompare (software) and found to be correct according to the placement and height. The lowest vertexes of the roofs of the LOD2 buildings are located on their correct locations compared with the TLS models. The visual inspection of the models is shown in Figure 11.

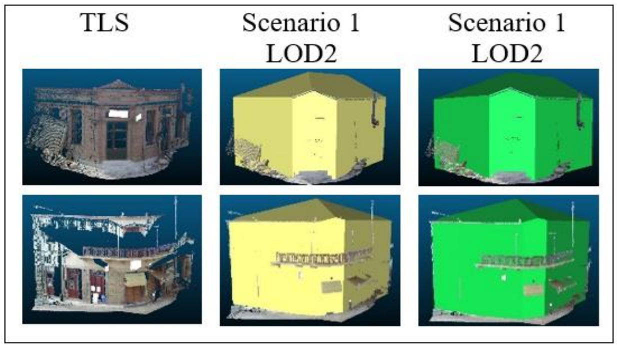

Figure 11. Example of visual inspection between two LOD2 Buildings and their corresponding TLS models

Moreover, a quantitative assessment was made for the comparison of the heights of the LOD2 buildings. TLS scans that took place during the 3D mapping of Vrisa settlement, produced dense point clouds with spatial resolution less than 1.5cm. TLS models are precise for measurements as they correspond to the actual sizes of the buildings. The heights of the buildings were measured from those TLS models and subsequently, were compared with the heights of the LOD2 buildings for both scenarios.

Figure 12. Comparison of heights between some TLS models and their corresponding LOD2 models of the two scenarios

The results are shown in Figure 12 and the values are very close between them. For some buildings, the height values are almost the same. This shows that the generation of LOD2 buildings is correct in terms of height.

4. CONCLUSIONS

In this study, two scenarios for the generation of LOD2 building models were investigated. LOD2 buildings generated with the utilization of UAS high-resolution images for monitoring the post-earthquake recovery phase of Vrisa settlement. The main difference between the two scenarios is the flying altitude which directly affects the spatial resolution of the information produced (DSM, orthophoto map) as well as the amount of information and their processing time. The two different scenarios consisted of two flight campaigns with different altitudes, one at 100 m and one at 40 m. The evaluation of the results, of the two scenarios, shows that the flying altitude does not significantly affect the reliability of the produced 3D models in LOD2.

For both scenarios, most of the LOD2 buildings were generated correctly, according to the results of the study, with the correct geometry and shape. Specifically, for the first scenario, 65 of the 80 LOD2 buildings were generated correctly and for the second the 64 respectively. In conclusion, in the case of 3D modelling of buildings in level of detail 2, it is preferable to choose a higher-flying altitude as it offers the advantages of smaller amount of data and processing time. This means that LOD2 buildings can be reconstructed correctly with a DSM of approximately 5 cm/pix spatial resolution and reliably footprints.

The BuildingReconstruction software, is appropriate for the automatic reconstruction of LOD2 building models, however, when dealing with complex roof shapes, or demolished and damaged buildings a manual model editing is necessary.

The 3D modelling of buildings after a natural disaster such as an earthquake offers excellent potential for the disaster management in the decision-making process to restore and rebuild the affected area. The developing of Citygml models in the disaster management can be useful for the storage, documentation, visualization and 3D mapping of an affected area.

In future work, a combination of oblique and nadir imagery will be exploited, for the data acquisition of the roofs and the facades of the buildings. Further attempts will be made, for the generation of LOD3 buildings, that will be enriched with the semantics of the damages. An improved CityGML model of a damage affected urban environment could be very helpful for stakeholders in damage assessment.

ACKNOWLEDGEMENTS

This research is co-financed by Greece and the European Union (European Social Fund- ESF) through the Operational Programme «Human Resources Development, Education and Lifelong Learning 2014-2020» in the context of the project “Development of 3D semantic models in 3D mapping and geo-visualization of earthquake effects in a traditional settlement” (MIS 5047141).

REFERENCES

Agisoft-LLC, 2020. Agisoft Metashape User Manual: Professional Edition, Version 1.6. Agisoft LLC.

Agugiaro, G., 2014: From sub-optimal datasets to a CityGML-compliant 3D city model: Experiences from Trento, Italy. *Int. Arch. Photogramm. Remote Sens. Spatial Inf. Sci*., XL-4, 7–13. https://doi.org/10.5194/isprsarchives-XL-4-7-2014

Biljecki, F., Stoter, J., Ledoux, H., Zlatanova, S., Çöltekin, A., 2015: Applications of 3D City Models: State of the Art Review. ISPRS *International Journal of Geo-Information* 4(4), 2842–2889. https://doi.org/10.3390/ijgi4042842

Buyukdemircioglu, M., Kocaman, S., Isikdag, U., 2018. Semi-automatic 3D city model generation from large-format aerial images. ISPRS *International Journal of Geo-Information* 7(9), p. 339. https://doi.org/10.3390/ijgi7090339

Chatzistamatis, S., Kalaitzis, P., Chaidas, K., Chatzitheodorou, C., Papadopoulou, E.E., Tataris, G., Soulakellis, N., 2018. Fusion of TLS and UAV photogrammetry data for post-earthquake 3D modeling of a cultural heritage church. *Int. Arch. Photogramm. Remote Sens. Spatial Inf. Sci.*, XLII-3/W4, 143–150. https://doi.org/https://doi.org/10.5194/isprs-archives-XLII-3-W4-143-2018

Chiabrando, F., Di Lolli, A., Patrucco, G., Spanò, A., Sammartano, G., Losè, L.T., 2017. Multitemporal 3D modelling for cultural heritage emergency during seismic events: Damage assessment of S. Agostino church in Amatrice (RI). *Int. Arch. Photogramm. Remote Sens. Spatial Inf. Sci.*, XLII-5/W1, 69–76. https://doi.org/10.5194/isprs-Archives-XLII-5-W1-69-2017

CloudCompare software. Available online: https://www.danielgm.net/cc/ (20 June 2020).

Daniyal, A., 2012. Post-Earthquake Damage Assessment using 3D-GIS Modeling, *in 33rd Canadian Symposium on Remote Sensing*.

Dominici, D., Alicandro, M., Rosciano, E., Massimi, V., 2017. Multiscale documentation and monitoring of l’aquila historical centre using uav photogrammetry. *Int. Arch. Photogramm. Remote Sens. Spatial Inf. Sci*., XLII-5/W1, 365–371. https://doi.org/10.5194/isprs-Archives-XLII-5-W1-365-2017

SAFE SOFTWARE 2015. ‘FME ® Desktop Manual’, pp. 1–378. Available online: http://docs.safe.com/fme_training/2015/pdf/FME_Desktop_Training_Manual.pdf

Gutmann, A. 2006. *On Risk and Disaster: Lessons from Hurricane Katrina* (DANIELS R., KETTL D., & KUNREUTHER H., Eds.). University of Pennsylvania Press.

Japan, G. O., WorldBank and GFDRR 2012. *The Sendai Report. Managing Disaster Risks for a Resilient Future.* Available at: www.worldbank.org.

Kada, M., McKinley, L., 2009. 3D building reconstruction from LiDAR based on a cell decomposition approach. *Int. Arch. Photogramm. Remote Sens. Spat. Inf. Sci*. 38(3), 47-52.

Khan, H., Vasilescu, L.G., Khan, A., 2008. Disaster Management Cycle – a Theoretical Approach. *Management and Marketing Journal*, 2008, 6(1), 43-50.

Kim, W., Kerle, N., Gerke, M., 2016. Mobile augmented reality in support of building damage and safety assessment. *Natural Hazards and Earth System Sciences*, 16, 287–298. https://doi.org/10.5194/nhess-16-287-2016

Kiratzi, A., 2018. The 12 June 2017 Mw 6.3 Lesvos Island (Aegean Sea) earthquake: Slip model and directivity estimated with finite-fault inversion. *Tectonophysics* 724–725, 1–10. https://doi.org/10.1016/j.tecto.2018.01.003

KIT, 2011. Karlsruhe Institute of Technology, Semantic Data Models, Available online at https://www.iai.kit.edu/english/1648.php (26 June 2020)

Kolbe T.H., Gröger G., Plümer L. 2005: CityGML: Interoperable Access to 3D City Models. In: van Oosterom P., Zlatanova S., Fendel E.M. (eds) *Geo-information for Disaster Management*. Springer, Berlin, Heidelberg

Kolbe T.H. 2009: Representing and Exchanging 3D City Models with CityGML. In: Lee J., Zlatanova S. (eds) *3D Geo-Information Sciences. Lecture Notes in Geoinformation and Cartography*. Springer, Berlin, Heidelberg

Lekkas, E., Mavroulis, S., Skourtsos, E., Andreadakis, E., Antoniou, V., Kranis, C., Soukis, K., Lozios, S., Alexoudi, V.,

2017. Earthquake environmental effects induced by the 2017 June 12, Mw 6.3 Lesvos (North Aegean Sea, Greece) earthquake, i*n 8th International INQUA Meeting on Paleoseismology, Active Tectonics and Archeoseismology (PATA)*, 232–235.

Letellier, R, Schmid, W., and Leblanc, F., 2007. Recording, Documentation, and Information Management for the Conservation of Heritage Places. Guiding Principles. The Getty Conservation Institute, Los Angeles, CA. http://hdl.handle.net/10020/gci_pubs/recordim

Ma, J., Qin, S., 2012. Automatic depicting algorithm of earthquake collapsed buildings with airborne high resolution image. In: *IEEE International Geoscience and Remote Sensing Symposium*, 939–942.

Maruyama, Y., Tashiro, A., Yamazaki, F., 2011. Use of digital surface model constructed from digital aerial images to detect collapsed buildings during earthquake. *Procedia Engineering*, 14, 552–558. https://doi.org/10.1016/j.proeng.2011.07.069

Open Geospatial Consortium, 2012. OGC City Geography Markup Language (CityGML) En-coding Standard 2.0.0. Technical Report.

Papadimitriou, P., Tselentis, G.A., Voulgaris, N., Kouskouna, V., Lagios, E., Kassaras, I., Kaviris, G., Pavlou, K., Sakkas, V., Moumoulidou, A., Karakonstantis, A., Kapetanidis, V., Sakkas, G., Kazantzidou, D., Aspiotis, T., Fountoulakis, I., Millas, C., Spingos, I., Lekkas, E., Antoniou, V., Mavroulis, S., Skourtsos, E., Andreadakis, E., 2017. Preliminary report on the Lesvos 12 June 2017 Mw=6.3 earthquake.

Papakonstantinou, A., Doukari, M., Roussou, O., Drolias, G., Chaidas, K., Moustakas, A., Athanasis, N., Topouzelis, K., Soulakellis, N., 2018. UAS multi-camera rig for post-earthquake damage 3D Geovisualization of Vrisa village, in *Sixth International Conference on Remote Sensing and Geoinformation of the Environment (RSCy2018)*. https://doi.org/https://doi.org/10.1117/12.2326173

Soulakellis, N., Chatzistamatis, S., Vasilakos, C., Tataris, G., Papakonstantinou, A., Kavroudakis, D., Topouzelis, K., Roussou, O., Kalloniatis, C., Papadopoulou, E.E., Chaidas, K., Kalaitzis, P., 2018. Synergistic exploitation of geoinformation methods for post-earthquake 3D mapping of Vrisa traditional settlement, Lesvos island, Greece, I*nt. Arch. Photogramm. Remote Sens. Spatial Inf. Sci*., XLII-3/W4, 491–498. https://doi.org/https://doi.org/10.5194/isprs-archives-XLII-3-W4-491-2018

Tang, L., Ying, S., Li, L., Biljecki, F., Zhu, H., Zhu, Y., Yang, F., Su, F., 2020. An application-driven LOD modeling paradigm for 3D building models. ISPRS *Journal of Photogrammetry and Remote Sensing,* 161, 194–207. https://doi.org/10.1016/j.isprsjprs.2020.01.019

Tu, J., Li, D., Feng, W., Han, Q., Sui, H., 2017. Detecting damaged building regions based on semantic scene change from multi-Temporal high-resolution remote sensing images. ISPRS *International Journal of Geo-Information* 6, 131. https://doi.org/10.3390/ijgi6050131

Virtualcity Systems Building Reconstruction. Available online: http://www.virtualcitysystems.de/en/products/buildingreconstruction (04 June 2020).

Xu, Z., Wu, L., Shen, Y., Li, F., Wang, Q., Wang, R., 2014. Tridimensional reconstruction applied to cultural heritage with the use of camera-equipped UAV and terrestrial laser scanner. *Remote Sensing*, 6, 10413–10434. https://doi.org/10.3390/rs61110413

Xu, Z., Yang, J., Peng, C., Wu, Y., Jiang, X., Li, R., Zheng, Y., Gao, Y., Liu, S., Tian, B., 2014. Development of an UAS for post-earthquake disaster surveying and its application in Ms7.0 Lushan Earthquake, Sichuan, China. *Computers and Geosciences*, 68, 22–30. https://doi.org/10.1016/j.cageo.2014.04.001

Yamazaki, F., Kubo, K., Tanabe, R., Liu, W., 2017. Damage assessment and 3d modeling by UAV flights after the 2016 Kumamoto, Japan earthquake, in IEEE *International Geoscience and Remote Sensing Symposium (IGARSS)*, 3182–3185. https://doi.org/10.1109/IGARSS.2017.8127673

YILMAZ, A., 2015. A framework for visualization of information in 3D virtual city environment for disaster management. PhD thesis, Middle East Technical University. http://etd.lib.metu.edu.tr/upload/12618877/index.pdf

Zheng, Y., Weng, Q., 2015. Model-Driven Reconstruction of 3-D Buildings Using LiDAR Data. IEEE *Geoscience and Remote Sensing Letters*, 12(7), 1541–1545. https://doi.org/10.1109/LGRS.2015.2412535